

## Polarization insensitivity electromagnetically induced reflection in graphene metasurface

WANG Jin<sup>1</sup>, WANG Xingchen<sup>1</sup>, GAO Xiang<sup>1</sup>, NING Renxia<sup>1,2</sup>

(1. School of Information Engineering, Huangshan University, Huangshan 245041, China;

2. Anhui Province Engineering Technology Research Center of Intelligent Microsystems, Huangshan 245041, China)

**Abstract:** The electromagnetically induced reflection (EIR) effect of graphene metamaterials has been investigated by finite difference time domain (FDTD) method. In this study, a metamaterial sandwich structure composed of silica (SiO<sub>2</sub>), gold and graphene on terahertz band is designed. By changing the width of the two ribbons of graphene length and the incident angle of electromagnetic wave, the EIR effect of the structure is discussed, and it can be found that SiO<sub>2</sub> is a kind of excellent dielectric material. The simulation results show that graphene metamaterial is not sensitive to polarized incident electromagnetic wave. Therefore, such EIR phenomena as insensitive polarization and large incident angle can be applied to optical communication filters and terahertz devices.

**Key words:** electromagnetically induced reflection (EIR); graphene metamaterials; polarization insensitivity; finite difference time domain (FDTD) method

### 0 Introduction

Electromagnetically induced transparency (EIT)<sup>[1]</sup> is a kind of destructive interference between energy levels in a three-level atomic system. It can induce sharp transparent windows in the frequency absorption region of the original opaque substance, and has better slow light effect and frequency selectivity. EIT phenomenon has been applied by optical storage<sup>[2]</sup>, sensing and switch devices<sup>[3]</sup>. In order to realize EIT in atomic system, the following conditions have been needed: precise selection of atomic energy level structure, two coherent light sources with higher light intensity, and experiments generally being carried out in a ultra-low temperature environment with complex experimental devices. These conditions limit its application in real life.

In recent years, the EIT effect has been introduced into metamaterials because some difficulties have been overcome and complex experimental conditions are realized in atomic systems<sup>[4]</sup>. Therefore, the use of various metamaterial structures to simulate the EIT phenomenon has become a new research focus<sup>[5-9]</sup>. At present, graphene metamaterial has attracted the

attention of researchers because of its ultra-thin and tunable properties<sup>[10]</sup>. Niu et al. studied a graphene-based T-shaped array metasurfaces and obtained tunable plasmon-induced transparency (PIT). By using the coupled Lorentz oscillator model to analyze the mechanism, it can be found that the PIT effect with the angle of incident is insensitive<sup>[11]</sup>. Liu et al. proposed a graphene metamaterial to realize analogue of dual-controlled EIT effect. By adjusting the incidence angle, the phase delay of the adjacent graphene patches changed and thus the frequency as well as the amplitude of transparency peak was modulated. Some of the above results provide a good reference for the realization of high-efficiency devices, such as modulators, switches, ultrashort pulse lasers, buffers and modulators with graphene material, etc.<sup>[12]</sup>

Electromagnetically induced reflection (EIR)<sup>[13]</sup>, as a kind of EIT-like phenomenon, has potential applications in sensing, optical communication and so on, which has attracted much attention in recent years. Liu et al. designed a dual-band infrared perfect absorber for plasmonic sensor based on the EIR-like

**Received date:** 2021-04-26

**Foundation items:** Research Project of Anhui Province Education Department (No. KJ2020A0684); Innovation and Entrepreneurship Training Program for College Students (Nos. S201910375072, 201910375050, 201910375052, 202010375030)

**Corresponding author:** NING Renxia (nrxxiner@hsu.edu.cn)

effect<sup>[14]</sup>. He et al. investigated graphene-based metamaterial featuring a dynamically tunable terahertz EIR, and the result can be applied to modulators, switches and slow light devices<sup>[15]</sup>. Jiang et al studied dynamic adjustable EIR in terahertz complementary graphene metamaterials. By changing the Fermi energy of graphene, the reflection window can be actively controlled, and the large positive group obtained in the reflection peak can be tuned in a wide terahertz region<sup>[16]</sup>. However, most researchers pay attention to the realization of EIR, but pay less attention to the EIR which is insensitive to polarization<sup>[17-18]</sup>.

In this study, we designed the graphene metamaterial on silicon-gold structure and analyzed the reflection spectra by finite difference time domain (FDTD) method. The length and width of graphene strips were changed to discuss the EIR effect. The results show that the structure has obvious polarization insensitive EIR phenomenon. This characteristic can be widely applied to many fields, such as sensors, filters and terahertz devices.

## 1 Model and design

To study EIR effect in the structure, reflection of the structure at normal incidence is analyzed, as shown in Fig. 1.

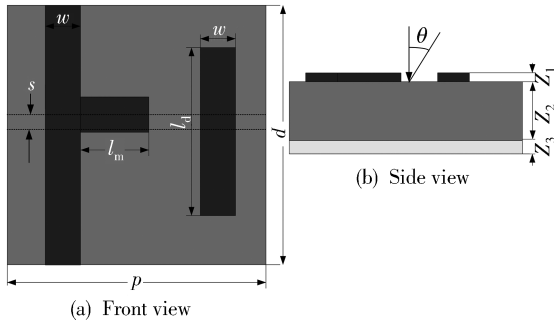


**Fig. 1 Unit cell of composite multilayer metasurface made by graphene-SiO<sub>2</sub>-Au with geometric parameters**

In Fig. 1,  $l_d=2.9 \mu\text{m}$ ,  $l_m=1.19 \mu\text{m}$ ,  $w=0.6 \mu\text{m}$ ,  $p=4.4 \mu\text{m}$ ,  $z_1=1 \mu\text{m}$ ,  $z_2=4 \mu\text{m}$ ,  $z_3=1 \text{nm}$ . The structure consists of three layers: a metallic plane layer on the bottom, a dielectric layer, and a layer with graphene strips. At the bottom of the substrate, the all-gold ground plane is at the bottom of the structure whose transmission is zero. As can be seen from Fig. 1,  $z_1$ ,  $z_2$  and  $z_3$  are the thicknesses of gold, the dielectric and graphene, respectively. The flexible dielectric can be chosen as SiO<sub>2</sub>, which is an ideal substrate material for graphene, here taking the

relative permittivity of the SiO<sub>2</sub> dielectric  $\epsilon = 3.9$ . Fig. 1 shows a horizontal graphene of length  $l_m$  with attached vertical graphene strip (T-shape) interacting with disconnected vertical graphene strip of length  $l_d$ . Assuming that the distance from horizontal graphene to the center of the unit structure is  $s$ , the periodic structures are illuminated by a normally incident plane wave and the incident angle of its electric field with respect to the  $x$ -axis is defined as  $\theta$  (see Fig. 1(b)), and perfectly matched layers (PML) are applied along the  $z$  direction and periodic boundary conditions in the  $x$  and  $y$  directions, the effective permittivity  $\epsilon_g$  of the graphene can be written as<sup>[19]</sup>

$$\epsilon_g = \frac{1 + i\sigma_g}{\epsilon_0 \omega z_3}, \quad (1)$$

where  $z_3$  is the thickness of graphene sheet,  $\epsilon_0$  is the permittivity in the vacuum,  $\sigma_g$  is the surface conductivity of graphene, and  $\omega$  is angular frequency.

For a graphene sheet, the electromagnetic properties can be described in terms of the  $\sigma_g$  that can be taken into account inter-band and intra-band transitions by Kubo model of conductivity<sup>[20-21]</sup>. The conductivity  $\sigma_g$  was derived using

$$\sigma_g = \frac{ie^2 k_B T}{\pi \hbar (\omega + i/\tau)} \left[ \frac{\mu}{k_B T} + 2 \ln(e^{-\frac{\mu}{k_B T}} + 1) \right] + \frac{ie^2}{4\pi \hbar} \ln \left| \frac{2\mu - \hbar(\omega + i/\tau)}{2\mu + \hbar(\omega + i/\tau)} \right|, \quad (2)$$

where  $\omega$  is radian frequency,  $\hbar$  is the reduced Planck constant,  $k_B$  is the Boltzman constant,  $e$  is the charge of an electron,  $T$  is the temperature,  $\mu$  is the chemical potential, and  $\tau$  is electron-phonon relaxation time.

The reflection spectra of the structure is shown in Fig. 2 on transverse electric (TE) and transverse magnetic (TM) mode at  $p=4.4 \mu\text{m}$ ,  $l_m=1.19 \mu\text{m}$ ,  $s=1.2 \mu\text{m}$ ,  $w=0.6 \mu\text{m}$ ,  $z_1=1 \mu\text{m}$ ,  $z_2=4 \mu\text{m}$ ,  $z_3=1 \text{nm}$  and  $l_d=2.9 \mu\text{m}$ . The reflection peak and valleys of TE mode are obtained on 5.309 1 THz, 5.115 2 THz and 5.536 2 THz, respectively. There are also two reflection valleys and one reflection peak of TM mode, corresponding to frequencies 5.115 2 THz, 5.536 2 THz and 5.309 1 THz, respectively. It is obvious from Fig. 2 that the peaks and valleys of the corresponding reflections on both TE and TM modes are at the same frequency. The simulation results show that the reflection of the structure is insensitive to polarization. It is noting that the structure is not the symmetry of  $x$  and  $y$  axis, so reflection on TE mode is smaller on TM

mode at the same frequencies.

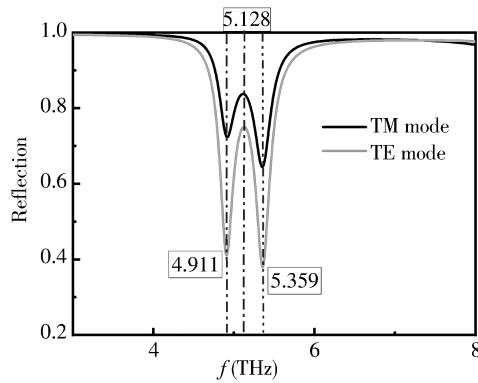


**Fig. 2 Comparison of reflection spectra of the structure on TE and TM mode**

To explain the result, we calculate the equivalent impedance. As shown in Fig. 3, the distance from horizontal graphene to the center of the unit structure is  $1.2 \mu\text{m}$ , the width of the graphene strip is  $0.6 \mu\text{m}$ , the length of the left graphene strip is  $2.9 \mu\text{m}$ , the intermediate material layer is  $\text{SiO}_2$ . It is demonstrated that the real part of equivalent impedance of the structure is smaller at  $5.1152 \text{ THz}$  and  $5.5362 \text{ THz}$ . The reason is that the bottom plate of the structure is made of gold, the energy transmitted is completely absorbed by the metal, and no energy is reflected back. The greater the equivalent impedance at a given frequency, the greater its ability to absorb energy and the lower the energy reflection.

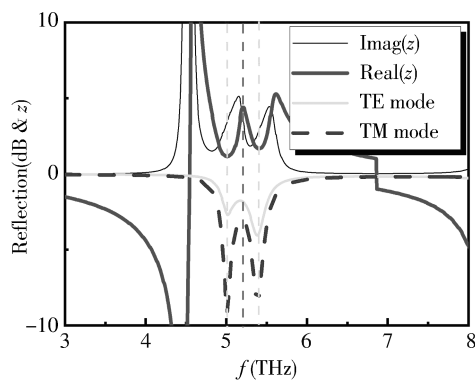


**Fig. 3 Equivalent impedance of the structure**

In order to better understand how the structure achieves polarization insensitivity, the following analysis is performed. Fig. 4(a) shows the electric field distribution for the proposed metamaterial. It is the electric field distribution for the proposed metamaterial at  $5.1152 \text{ THz}$ ,  $5.3091 \text{ THz}$  and  $5.5362 \text{ THz}$ . On TE mode, it can be observed that the concentration of power loss distribution for  $5.1152 \text{ THz}$  and  $5.3091 \text{ THz}$  are the highest at the horizontal graphene in the middle of the structure.

However, on TM mode, the distribution of electric field at frequencies of  $5.1152 \text{ THz}$  and  $5.3091 \text{ THz}$  are different from those on TE mode. The electric field is mainly distributed at the upper and lower edges of the vertical graphene strip on the left side of the structure. When the frequency is  $5.5362 \text{ THz}$ , the distribution of electric field on TE and TM modes is opposite to those of the above two frequencies. On TE mode, the electric field is concentrated in the left vertical graphene strip. The electric field is concentrated on the middle horizontal graphene strip on TM mode. In Fig. 4(b), the magnetic-field pattern indicates that in the case of  $5.3091 \text{ THz}$  and  $5.5362 \text{ THz}$ , the magnetic field is mainly distributed in the middle of the left vertical graphene and at the junction of the horizontal graphene and the vertical strip graphene on the right. On TE mode, as the frequency increases, the intensity of the magnetic field decreases at the center of the left vertical graphene band, but increases gradually at the right joint of horizontal graphene. The distribution of the magnetic field on TM mode is different from the above. The magnetic field decreases on the horizontal graphene strip and increases on the left vertical graphene strip.

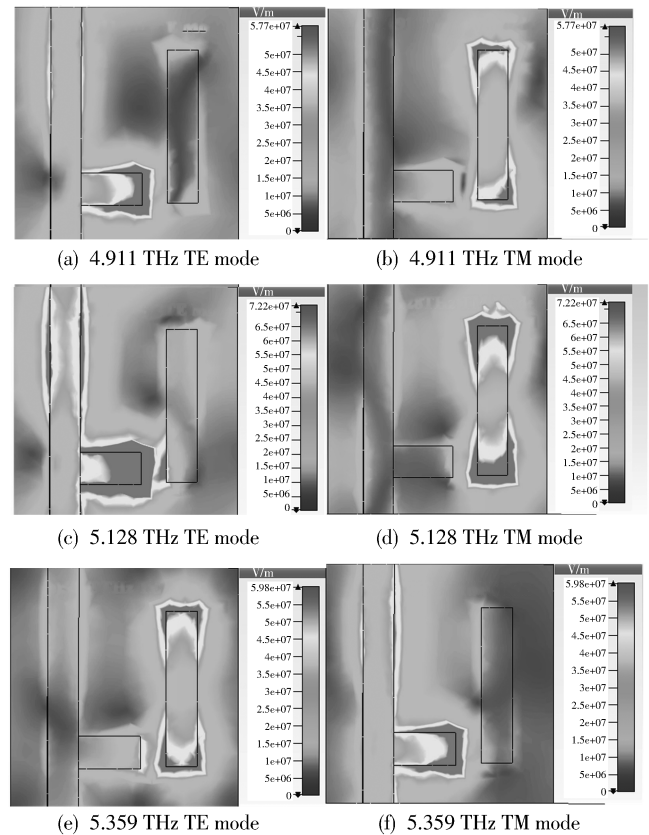


**Fig. 4 Electric field distribution at reflection peak frequency of  $5.3091 \text{ THz}$  and reflection valleys frequencies of  $5.1152 \text{ THz}$  and  $5.5362 \text{ THz}$**

## 2 Results and discussion

To further study the reflection of structure, we adjust vertical graphene strip of length  $l_d$  as follows:  $l_d = 2.7 \mu\text{m}$ ,  $2.8 \mu\text{m}$ ,  $2.9 \mu\text{m}$ , and  $3 \mu\text{m}$ , respectively, and the other parameters are consistent with Figs. 2 and 3, namely,  $p = 4.4 \mu\text{m}$ ,  $l_m = 1.19 \mu\text{m}$ ,  $s = 1.2 \mu\text{m}$ ,  $w = 0.6 \mu\text{m}$ ,  $z_1 = 1 \mu\text{m}$ ,  $z_2 = 4 \mu\text{m}$  and  $z_3 = 0.01 \mu\text{m}$ . The results show that there is one reflectivity peak and two reflectivity valleys at different  $l_d$ . It is clearly shown that in TE mode, as the  $l_d$  changes from  $2.7 \mu\text{m}$  to  $3 \mu\text{m}$ , the reflection spectra of the TE mode is produces red shift. It can be seen from Fig. 5 that the reflection valley is a shifted-red at increasing  $l_d$ . The reflection of the low frequency is gradually strengthened and the reflection of the high frequency is gradually weakened. Similar results occurs in TM mode, where increasing  $l_d$  changes the resonant frequency and reflection. On the contrary, the reflection of low frequency is larger and smaller on high frequency.

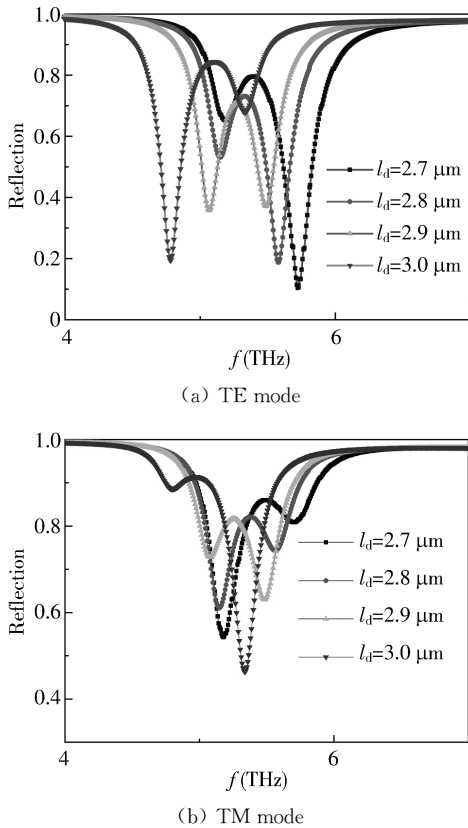


Fig. 5 Reflection spectra change in variation of  $l_d$

We change the distance of the horizontal graphene strip to the center of the structure  $s$  varied from  $0.7 \mu\text{m}$  to  $1.5 \mu\text{m}$ , as shown in Fig. 6, and other parameters in the structure are  $p = 4.4 \mu\text{m}$ ,  $l_d = 2.9 \mu\text{m}$ ,  $l_m = 1.19 \mu\text{m}$  and  $w = 0.6 \mu\text{m}$ . The results show

that the reflection decreases and the frequency at reflection peaks is almost unchanged when  $s$  is  $0.7 \mu\text{m}$  to  $1.5 \mu\text{m}$ , respectively. It can be seen that the change of reflection peaks and reflection valleys of the reflection spectrum is small in frequency range no matter how  $s$  changes. The symmetry of the structure can be broken as long as the strip graphene is not in the center. EIR effect can be found at  $s$  being not zero.

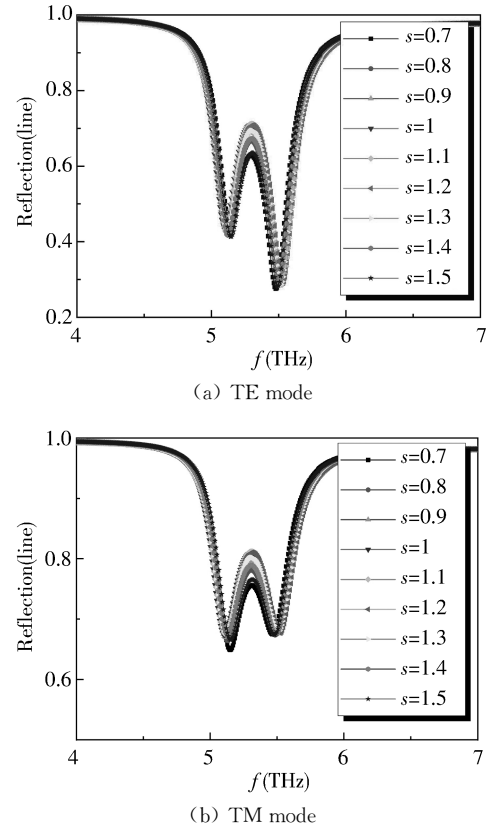
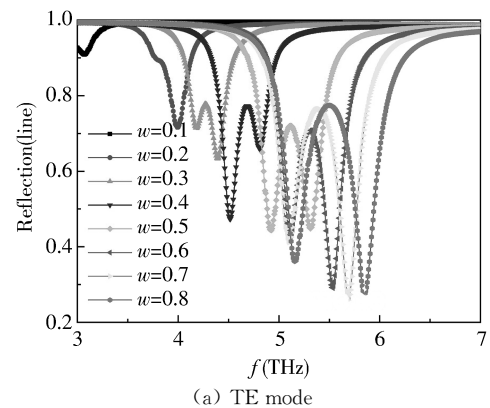


Fig. 6 Change of reflectance spectra with changed  $s$

The reflection spectrum of the structure is studied by changing the width of the graphene strip  $w$  and other parameters in the structure are  $p = 4.4 \mu\text{m}$ ,  $l_d = 2.885 \mu\text{m}$ ,  $l_m = 1.19 \mu\text{m}$  and  $s = 1.2 \mu\text{m}$ . It can be seen that the reflection peaks and troughs of the reflection spectrum occur red shift in Fig. 7.



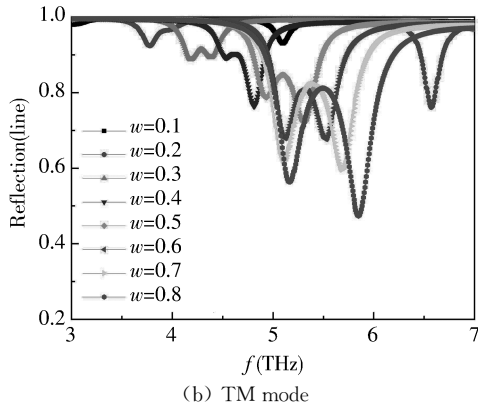


Fig. 7 Change with reflection spectra of different  $w$

In addition, no matter in the TE mode or TM mode, it can be clearly seen that the resonance frequency decreases with the decrease of the width  $w$  of the graphene band. On the contrary, the reflection value increases under the same condition. It is worth nothing that the EIR effect is very weak at  $w = 0.2 \mu\text{m}$  on TE mode and TM mode. When  $w = 0.1 \mu\text{m}$ , the EIR phenomenon on TE mode basically disappears. The EIR effect of the structure is obtained by the coupling of two graphene strips. The smaller the length of  $w$  of the coupling between the two graphene strips weak. And the EIR phenomenon disappears.

Next, we study the EIR of the structure by changing the incident angle, and plot the reflection spectra of different angle, as shown in Fig. 8. Assuming that angle changes from  $0^\circ$  to  $75^\circ$ , we can see that changing the angle do not shift the reflected peaks and the corresponding frequencies. However, it can be seen that the variation of the incident angle results in the decrease of the reflection value of the peaks in TE mode. As the angle of incidence gradually increases, the shift of smaller trough reflection occurs in TE and TM modes. As the angle increases, the component becomes smaller in  $z$ -axis direction.

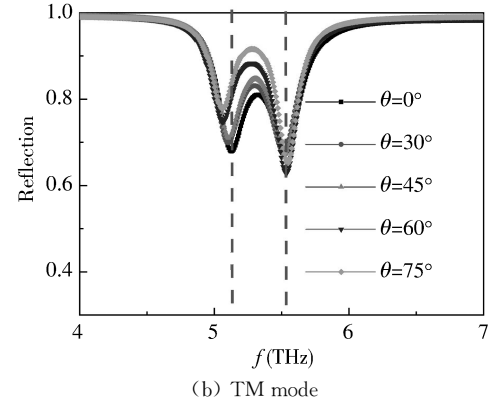
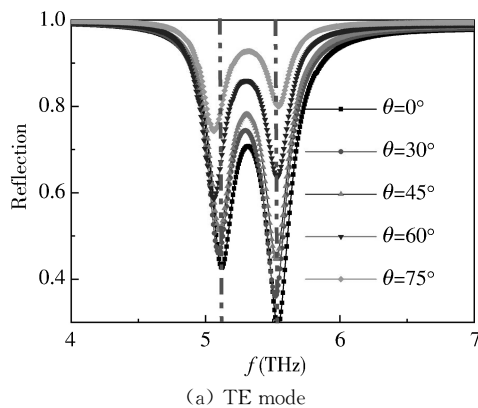


Fig. 8 Change with reflection spectra of different  $\theta$ , from  $0^\circ$  to  $75^\circ$

Finally, we use  $\text{Si}_3\text{N}_4$  instead of  $\text{SiO}_2$  as the dielectric material. The reflection spectrum of  $\text{Si}_3\text{N}_4$  is shown in Fig. 9. Compared with  $\text{SiO}_2$ , there are also two reflection valleys and one reflection peak, corresponding to frequencies 4.888 1 THz, 5.303 6 THz and 5.087 5 THz. Therefore, it is obvious from Fig. 9 that the peaks and valleys of the corresponding reflections on both TE and TM modes are at the same frequency. The results show that the structure is insensitive to polarization. Changing the material of  $\text{Si}_3\text{N}_4$  and  $\text{SiO}_2$  has no obvious effect on reflection. However, the frequency of reflection peak shows a blue shift with  $\text{Si}_3\text{N}_4$ .

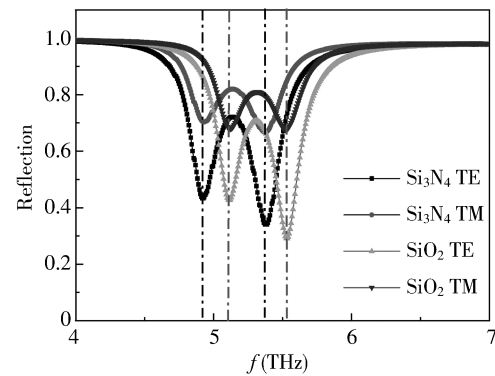


Fig. 9 Comparison with reflection spectra of the structure with different dielectric layer, with media of  $\text{SiO}_2$  and  $\text{Si}_3\text{N}_4$

### 3 Conclusions

In summary, a polarization insensitive metamaterial of graphene has been designed. The reflection properties of the metamaterials are observed at different widths and lengths of graphene strips. We change the incident angle to discuss the influence of the electric field distribution of graphene strip. The results show that the three-layer structure can achieve polarization insensitivity and EIR on large incident angle. We study the effect of different

materials on structural polarization insensitivity. It can be concluded that the graphene metamaterial structure is not sensitive to polarization of the incident electromagnetic wave. In order to understand the physical reasons for the insensitivity of this structure to polarization, we have studied the distribution of electric and magnetic fields at special frequencies. The results can be valuable in applications on optical communication, filter and terahertz devices.

## References

- [1] Xia H, Sharpe S J, Merriam A J, et al. Electromagnetically induced transparency in atoms with hyperfine structure. *Physical Review A*, 1997, 56(5): 315-319.
- [2] Heinze G, Hubrich C, Halfmann T. Stopped light and image storage by electromagnetically induced transparency up to the regime of one minute. *Physical Review Letters*, 2013, 111(3): 033601.
- [3] Liu N, Weiss T, Mesch M, et al. Planar metamaterial analogue of electromagnetically induced transparency for plasmonic sensing. *Nano Letters*, 2010, 10(4): 1103-1107.
- [4] Papasimakis N, Fedotov V A, Zheludev N I, et al. Metamaterial analog of electromagnetically induced transparency. *Physical Review Letters*, 2008, 101(25): 253903.
- [5] Shu C, Chen Q G, Mei J S, et al. Dynamically tunable implementation of electromagnetically induced transparency with two coupling graphene-nanostrips in terahertz region. *Optics Communications*, 2018, 411: 48-52.
- [6] Tang H, Zhou L, Xie J, et al. Electromagnetically induced transparency in a silicon self-coupled optical waveguide. *Journal of Lightwave Technology*, 2018, 36(11): 2188-2195.
- [7] Wang Y, Leng Y, Wang L, et al. Broadband tunable electromagnetically induced transparency analogue metamaterials based on graphene in terahertz band. *Applied Physics Express*, 2018, 11(6): 062001.
- [8] Xiao S, Wang T, Liu T, et al. Active modulation of electromagnetically induced transparency analogue in terahertz hybrid metal-graphene metamaterials. *Carbon*, 2017, 126: 271-278.
- [9] Shen Z Y, Xiang T Y, Wu N, et al. Dual-band electromagnetically induced transparency based on electric dipole-quadrupole coupling in metamaterials. *Journal of Physics D: Applied Physics*, 2018, 52(1): 015003.
- [10] Luo W, Cai W, Xiang Y, et al. Flexible modulation of plasmon-induced transparency in a strongly coupled graphene grating-sheet system. *Optics Express*, 2016, 24(6): 5784-5793.
- [11] Niu Y, Wang J, Hu Z, et al. Tunable plasmon-induced transparency with graphene-based T-shaped array metasurfaces. *Optics Communications*, 2018, 416: 77-83.
- [12] Liu C X, Liu P G, Yang C, et al. Analogue of dual-controlled electromagnetically induced transparency based on a graphene metamaterial. *Carbon*, 2019, 142: 354-362.
- [13] Vafapour Z. Large group delay in a microwave metamaterial analog of electromagnetically induced reflectance. *Journal of the Optical Society of America A*, 2018, 35(3): 417-422.
- [14] Liu Y, Zhang Y Q, Jin X R, et al. Dual-band infrared perfect absorber for plasmonic sensor based on the electromagnetically induced reflection-like effect. *Optics Communications*, 2016, 371: 173-177.
- [15] He X, Yao Y, Huang Y, et al. Active manipulation of electromagnetically induced reflection in complementary terahertz graphene metamaterial. *Optics Communications*, 2018, 407: 386-391.
- [16] Jiang J, Zhang Q, Ma Q, et al. Dynamically tunable electromagnetically induced reflection in terahertz complementary graphene metamaterials. *Optical Materials Express*, 2015, 5(9): 1962-1971.
- [17] Shen Z, Xiang T, Wu J, et al. Tunable and polarization insensitive electromagnetically induced transparency using planar metamaterial. *Journal of Magnetism and Magnetic Materials*, 2019, 476: 69-74.
- [18] Li H. Polarization-insensitive electromagnetically induced transparency based on ultra-thin coupling planar metamaterials. *Optical Materials Express*, 2018, 8(2): 348-355.
- [19] Ning R X, Bao J, Meng Y J, et al. Wideband reciprocity tunable electromagnetically induced transparency in complementary graphene metasurface. *Journal of Optics*, 2019, 21: 045106.
- [20] Mikhailov S A, Ziegler K. A new electromagnetic mode in graphene. *Physical Review Letters*, 2007, 99(1) : 016803.
- [21] Falkovsky, L A. Optical properties of graphene. *Journal of Physics Conference Series*, 2008, 129: 012004.

## 石墨烯超表面的极化不敏感电磁诱导反射

王 瑾<sup>1</sup>, 汪星辰<sup>1</sup>, 高 翔<sup>1</sup>, 宁仁霞<sup>1,2</sup>

(1. 黄山学院 信息工程学院, 安徽 黄山 245041;

2. 安徽省智能微系统工程技术研究中心, 安徽 黄山 245041)

**摘 要:** 利用时域有限差分(Finite difference time domain, FDTD)方法研究了石墨烯超材料的电磁诱导反射(Electromagnetically induced reflection, EIR)效应。首先,设计了一种在太赫兹波段上由二氧化硅( $\text{SiO}_2$ )、金和石墨烯条组成的三层超材料结构。然后,讨论了石墨烯条的宽度、长度和电磁波的入射角等参数不同的情况下该结构的电磁诱导反射效应,并通过改变结构的中间层介质材料得出  $\text{SiO}_2$  是一种优良的介电材料。最终的模拟结果表明,该石墨烯超材料对极化入射的电磁波不敏感。该极化不敏感和大入射角的电磁诱导反射结构在光通信滤波器和太赫兹器件中有潜在的应用。

**关键词:** 电磁诱导反射; 石墨烯超材料; 极化不敏感; 时域有限差分法

**引用格式:** WANG Jin, WANG Xingchen, GAO Xiang, et al. Polarization insensitivity electromagnetically induced reflection in graphene metasurface. Journal of Measurement Science and Instrumentation, 2021, 12(3): 362-368. DOI: 10.3969/j.issn.1674-8042.2021.03.015